Received: 13 March 2018 | Revised: 22 June 2018 | Accepted: 10 July 2018

DOI: 10.1002/ett.3498

SPECIAL ISSUE ARTICLE

WILEY

Implementation of a VLC-based indoor localization system

E. Torres-Zapata[1] | J. M. Luna-Rivera[1] | R. Perez-Jimenez[2] | V. Guerra[2] | J. Rabadan[2] | J. Rufo[2] | C. A. Gutierrez[1]

[1]Facultad de Ciencias, Universidad Autónoma de San Luis Potosí, San Luis Potosí, México

[2]IDeTIC, Universidad de las Palmas de Gran Canaria, Las Palmas, Gran Canaria, Spain

Correspondence
J. M. Luna-Rivera, Facultad de Ciencias, UASLP, Av. Salvador Nava s/n, Zona Universitaria, C.P. 78290, San Luis Potosí, México.
Email: mlr@uaslp.mx

Present Address
Av. Salvador Nava s/n, Zona Universitaria, C.P. 78290, San Luis Potosí, S.L.P., México

Funding information
CONACYT, Mexico, Grant/Award Number: 236188; Spanish Government (Economy, Industry and Competitiveness Ministry), Grant/Award Number: TEC2013-47682-C2-1

Abstract

Nowadays, with the incursion of solid state lighting technology in our daily life, visible light communication (VLC) systems are becoming more important. This fact has generated a lot of attention on VLC to provide solutions on multiple applications where this technology can be exploited. At the same time, the growing of automation processes has created the necessity of knowing the localization of different objects and devices. Indoor localization based on radio frequency signals is one of the most used techniques (Wi-Fi, Bluetooth, UWB, RFID, etc); however, VLC is a new and interesting method, which is gaining enormous research attention. Moreover, there are environments where the use of RF technologies is restricted or even prohibited. In such cases, VLC technology becomes an interesting alternative to solve this problem. In this paper, we design and implement a novel VLC-based indoor localization system that combines the application of a VLC scheme for downlink and an ultrasonic communication for the uplink. Practical localization experiments are carried out in an actual office room environment, and results show a localization accuracy of 4 cm on average for direct links and 10 cm for indirect links.

1 | INTRODUCTION

In recent years, the rise of mobile devices and the excessive demand for data have caused the saturation of the electromagnetic spectrum. This trend has led to the search for new communication alternatives to meet such demands, among these options is the use of an innovative mean of transmitting data called visible light communication (VLC). Moreover, VLC technology adopts the visible light between 375 and 780 nm to transmit data wirelessly. Because LEDs are solid-state lighting devices, they can be modulated at a high speed, which avoids to be detected by the human eye and enabling it for the dual purpose of data communication and illumination simultaneously. Inherent features of VLC include energy efficiency, high bandwidth available, not being affected by electromagnetic interference, as well as having a robust security. These factors have led to significant interest in VLC with the potential to provide a contribution to the short-range communication demands. Potential applications of VLC include vehicle-to-vehicle communication, consumer electronics, healthcare, home and building automation, robots in hospitals, underwater communication, information displayed on sign boards, etc.[1]

Location-based services have particularly become a very important topic for indoor wireless communications. With the incursion more and more of automated processes, as well as the appearance of the Internet of Things, there is a growing demand for location awareness in many Internet of Things applications. The most extended localization technology is the Global Positioning System, which allows determining the location of an object with a standard accuracy up to a few meters.

However, the main drawback is that such accuracies can only be achieved in outdoor environments. As the location services market continues to grow, the deployment of Indoor Positioning Systems (IPS) opens up plenty of possibilities to drive new mobile applications. In response to this demand, a number of different technologies have been studied for the indoor positioning market, including bluetooh proximity, based beacon tags, and WiFi-, ultra narrow band-, acoustic-, or infrared-based systems. Despite these current technologies, the indoor positioning market is still in early stages, and there are alternative position-determination systems that need to be addressed.[2] Furthermore, there are environments such as petrochemical plants, hospitals, manufacturing plants, airports, underground mines, underwater, etc, where the use of radio frequency (RF) is not wanted, not secure, or actually impossible.[3-5] In this way, the confined nature of light propagation in indoor environments makes VLC-based IPS a promising technology to deliver a variety of location-based services to networked wireless devices.

The development of IPS based on VLC has several important challenges. One of them is dealing with the simplex communication for VLC; sometimes it needs to be complemented by additional technologies such as ultrasound or RF, for supporting the distance measurements (for example in TDOA schemes) or data transmission and network connection (WiFi). Moreover, it also deals with the relation between accuracy on localization and the complexity of the method. When the method used requires additional information, it demands high computing resources or extend setup processes. Further relevant issues are those related to the problems of VLC systems like the reliability on the communication link, the range of the link, the noise of the environment, and so forth.

Several research groups are working on indoor positioning using VLC, the most frequently solution is the application of the trilateration method using the received signal strength intensity (RSSI) value for distance measurements. Some of these proposals are used together with frequency ID to distinguish the emitting sources. This frequency ID process consists of transmitting a modulated signal, which has a different carrier signal for each node.[6-9] An advantage of this process is that the receiver can obtain reference points for the minimum and maximum power of the signal, which makes it useful for canceling the environment's light. This method has a good precision range without additional hardware. However, on the other hand, it can be very sensitive to the movements of the receiver, which increases significantly the error range. Moreover, the error grows up in scenarios with very tall lamps (more than 1.5-m high).[10] There are some others works in the literature that combine RSSI-based technique with other additional methods to minimize these effects, for example triangulation.[7] For this, it is necessary to modify the hardware at the transmitter to provide angle information, where the transmitter emits multiple signals at the same time.

Other method often employed is the scene analysis. This method needs to characterize the features of the environment before applying the localization process. On a setup stage, different measurements are collected in the room, where the system operates. The collected information is called fingerprint. After this stage, an existing localization algorithm is performed using the collected fingerprint information to improve the results. One example of working with fingerprints is presented in the work of Guo et al[8]; on the setup process, the RSSI is measured on different points of the room. Each measure is represented as a signal or function of time with a significant number of samples. Then, these samples are transformed into the frequency domain and stored on a database. The database is used as a reference for the localization problem. When the localization process is ongoing, the hardware needs to collect the RSSI information and transform to frequency domain. This information provides a frequency ID for the optical sources in the localization system, which are then compensated with the database fingerprints to mitigate the environment distortions. With a similar methodology, the works of Qiu et al[11,12] create a spatial probability distribution function of the environment and then uses Bayesian filtering to determinate the localization point with the highest probability.

Other type of IPS based on VLC technology employs cameras as receiver. For example, in the work of Huynh et al,[13] the collected images by the camera are used to calculate the distance between the transmitter and the receiver. The accuracy of the results are dependent of image resolution, with more pixels per image less error, but it requires more processing time.

This paper proposes a VLC-based method for indoor localization that uses the results of a distance-based trilateration technique. We follow our approach in the work of Marin-Garcia et al[14] for distance estimation, which takes advantage of the difference in propagation speeds of two signals in a medium. It analyzes the practical aspects of this kind of systems and proposed some ideas for solving some of the problems found in a real scenario such as noise or time schedule of the round-trip time of flight (RTOF) distance measurement. In this way, the proposed system provides a more accurate approach for the distance estimation than RSSI or scene analysis methods. Furthermore, it does not need complex computational processes or databases access as in camera-based systems or based on fingerprints. Thus, we present the implementation of an indoor localization system by using the estimated distances and solving the trilateration problem. This validation provides practical insights on the indoor positioning performance using VLC and identify some of the challenges and future phases of this type of systems.

The reminder of this paper is organized as follows. Section 2 describes the architecture of the proposed localization system. Explanation of hardware implementation is discussed in Section 3. Section 4 presents the results of the validation process. Finally, Section 5 discusses the conclusions and future work.

2 | PROPOSED VLC-BASED LOCALIZATION SYSTEM

Figure 1 shows the conceptual representation of the proposed VLC-based localization system. It assumes a group of static LED luminaires (nodes L) and one mobile device (node M). For this localization problem, the objective is to obtain the position of the node M by using distance measurements among some of the nodes L and node M. A direct real-time solution to determine such distances consists on measuring the time of flight of the signal from node M to node L and back, referred as round-trip time of flight. With the distance used as a radius, a circular representation of the area around a node L is constructed for which the position of the node M is highly probable. Figure 2 illustrates the indoor localization concept with a distance-based trilateration approach using RTOF. Without loss of generality, we resolve the node M position in two dimensions, ie, assuming that the distances from three of nodes L are available. Three-dimensional resolution can be performed by constructing spherical instead of circular models.

The distance between the nodes L and M is estimated by taking advantage of the difference in propagation speeds of an optical signal (speed of light), used for the downlink (node L to node M), and an ultrasound signal (speed of sound), used for the uplink (node M to node L). Figure 3 shows a simplified block diagram of the integrated VLC-based communication system to carry out the process of distance measurements. From knowledge of both propagation speeds and measured times, distance can be calculated as follows:

$$\tilde{D} = \frac{c \cdot v_s}{c - v_s}\Delta t \underset{c>>v_s}{\approx} v_s \cdot \Delta t, \tag{1}$$

where $\tilde{D}$ defines the distance from node L to node M, Δt is the time delay, c is the speed of light, and v_s is the speed of sound, which depends on the temperature of the room.

FIGURE 1 Conceptual representation of the visible light communication–based localization system

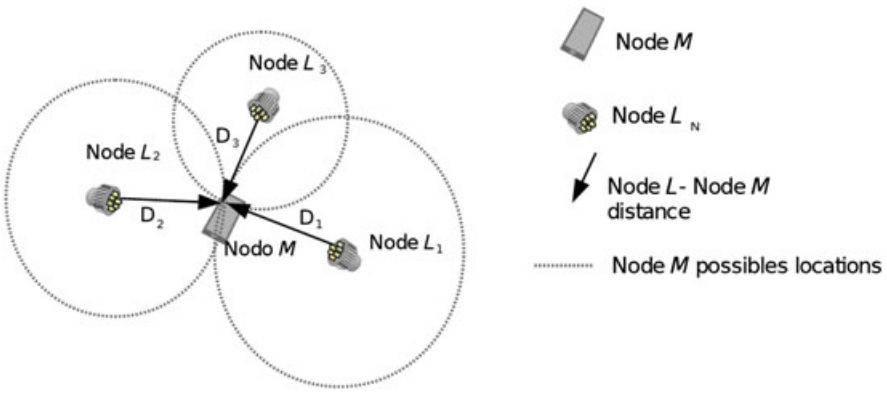

FIGURE 2 Illustration of the trilateration method using round-trip time of flight–based distance measurements

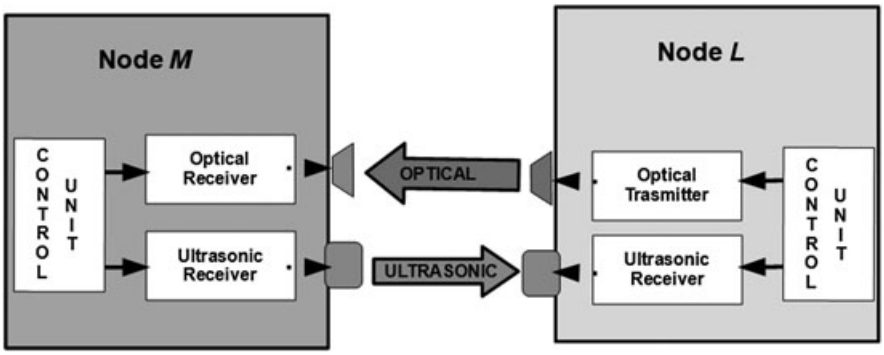

FIGURE 3 Block diagram for the communication links between node *M* and node *L*

2.1 | RTOF-based distance measurements

In addition, RTOF like time of flight technique is based on the intersection of circumferences which radius are the calculated distance from the node *M* to the nodes *L*. In the first phase of the proposed VLC-based localization system, node *M* initiates the process by sending an ultrasonic pulse to the nodes *L* in the room. Once these nodes detect the ultrasonic signal, they transmit an optical signal back to node *M* with the objective of estimating the RTOF. Next, a trilateration method is performed for indoor localization at the node *M* using RTOF-based distance measurements.

The RTOF process described in Figure 4 is summarized through the following six steps:

1. At the instant t_0, node *M* initiates the communication by transmitting the ultrasonic signal $V_{tx}^{\text{us}}(t)$.
2. At the instant t_1, node *L* initiates the detection of the ultrasonic signal sent by the node *M*, where $t_{rx}^{p} = |t_2 - t_1|$ defines the processing time required by the receiver to detect the signal. The propagation time of the ultrasonic signal between node *M* and node *L* is described as $t_{tx}^{\text{us}} = |t_1 - t_0|$.
3. Each node *L* maintains a waiting time, $t_{r,L} = |t_3 - t_2|$ before starting the optical transmission which helps to avoid collisions on the optical channel. This variable reduces the collision probability of the optical signals transmitted from all the nodes *L*.
4. At the instant t_3, the node *L* responds to the communication of the node *M* by transmitting back with the optical signal $V_{tx}^{\text{opt}}(t)$.
5. The node *M* detects and processes the optical signal sent by the node *L* during the interval $|t_4 - t_3|$.
6. Finally, from time t_4, the control unit of node *M* processes the measured distances from at least three of the references nodes to estimate its location using the trilateration method. In this case, the interval $t_i = |t_5 - t_4|$ determines the time that the node *M* takes to perform the trilateration method.

Taking the start of the ultrasonic signal transmission as the reference time t_0, the ultrasonic signal received at the node *L* can be expressed as

$$V_{\text{us}}(t) = V_{tx}^{\text{us}}(t) * h_{tx}^{\text{us}}(t) * h_{ch}^{\text{us}}(t) * h_{rx}^{\text{us}}(t) + n^{us}(t), \tag{2}$$

where $*$ defines the convolution operator, $V_{tx}^{\text{us}}(t)$ is the ultrasonic excitation signal, $h_{tx}^{\text{us}}(t)$ is the impulse response of the transmitter, $h_{ch}^{\text{us}}(t)$ denotes the ultrasonic channel impulse response, $h_{rx}^{\text{us}}(t)$ is the impulse response of the receiver, and

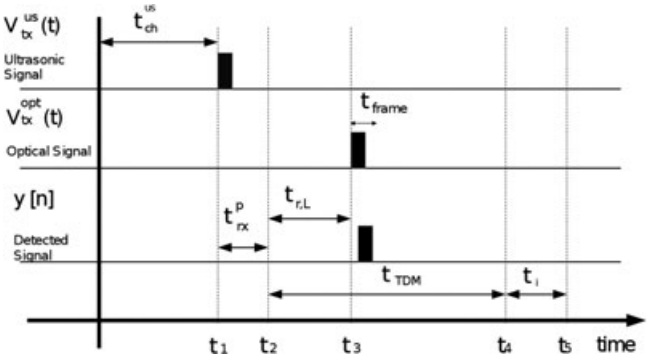

FIGURE 4 Operational schedule for round-trip time of flight–based distance measurements

$n^{\text{us}}(t)$ the additive noise signal at the receiver. Finally, the arrival instant of the signal for a given threshold level V_{th} can be expressed as

$$t_{\text{arrival}} = \arg\min_{t}\{V_{rx}(t) > V_{th}\}. \tag{3}$$

Note that the above equation makes sense only for rising edge detection. Moreover, if any of the elements produced a nonlinear distortion, Equation (3) would remain valid, whereas Equation (2) should change accordingly. Similar to Equation (2), the optical communication link from node L to node M can be written as

$$V_{\text{opt}}(t) = V_{tx}^{\text{opt}}(t) * h_{tx}^{\text{opt}}(t) * h_{ch}^{\text{opt}}(t) * h_{rx}^{\text{opt}}(t) + n^{\text{opt}}(t), \tag{4}$$

where $V_{tx}^{\text{opt}}(t)$ is the optical excitation signal and $h_{tx}^{\text{opt}}(t)$ and $h_{rx}^{\text{opt}}(t)$ are the impulse responses of the optical transmitter and receiver chains, respectively. The impulse response of the indoor VLC channel is denoted as $h_{ch}^{\text{opt}}(t)$ and the additive noise source at the receiver as $n^{\text{opt}}(t)$. We remark that before transmitting the optical excitation signal in step 4, $V_{tx}^{\text{opt}}(t)$, there is a waiting time $t_{r,L}$ for each node L, see Figure 4. In other words, the implemented system makes use of a type of time division multiplexing scheme to avoid collisions since all reference nodes share the same optical channel. The time $t_{r,L}$ is fixed and different for each node; this time information is sent on the optical signal.

Finally, Figures 5 and 6 show the flowchart representations for the sequence of process steps for both node M and node L. In summary, Figure 5 shows that node M starts the process by transmitting the ultrasonic signal $V_{tx}^{\text{us}}(t)$. Then, it waits until an optical signal, $V_{tx}^{\text{opt}}(t)$, has been sent by one of the nodes L. If an optical data frame is detected, then node M estimates the time of arrival t; otherwise, it waits until an optical signal arrives. The next step is to verify the condition $t < t_4$; if it is true, the counter for the number of data frames detected is increased. If the number of data frames detected is equal or greater than 3, then the trilateration method is performed to calculate the position of node M.

On the other hand, Figure 6 gives a step by step procedure for each of the nodes L. First, nodes L are sensing the channel until the ultrasonic signal sent by node M arrives. Then, there is a waiting time $t_{r,L}$ before starting the transmission of the optical signal $V_{tx}^{\text{opt}}(t)$. This contention time is different for each node L, and it allows the introduction of a sort of multiple access scheme in the system to reduce the collision probability of the optical signals from the other nodes L. Next, each node L transmits back the optical signal toward the node M when the contention time ends. Finally, the optical signal transmission ends and the process starts again.

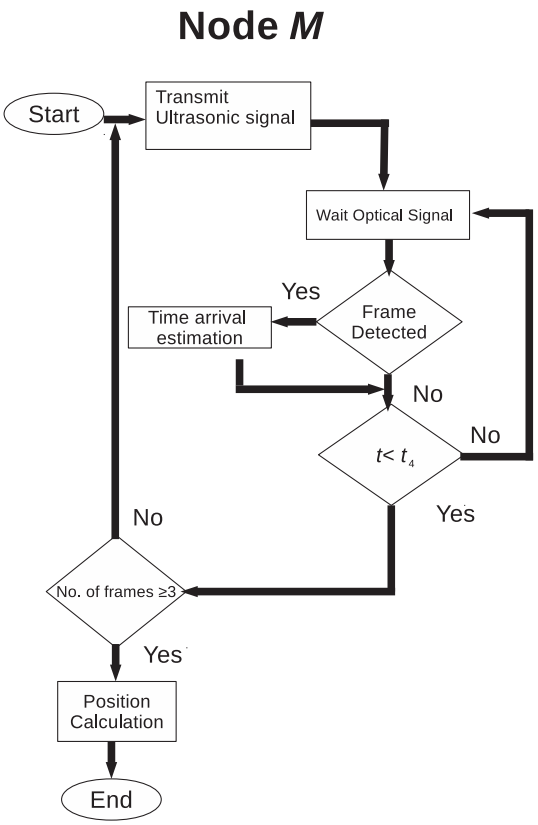

FIGURE 5 Flowchart for the sequence of process steps at node M

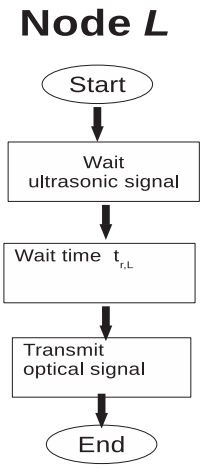

FIGURE 6 Flowchart for the sequence of process steps at node *L*

2.2 | Distance measurement errors

In addition, RTOF-based distance measurement is sensitive to different error sources. As the aforementioned procedure suggests, time measurement errors due to source jitter or receiver noise may generate distance estimation errors. Furthermore, since acoustic signal propagation depends on factors such as temperature and pressure, inaccurate estimations of these parameters may produce a harmful effect on the estimated distance measure.

The distance estimation error is the difference between the actual distance, D, and the RTOF-based distance estimation, which can be defined as

$$\epsilon = D - v_s \cdot \Delta t. \tag{5}$$

As it is shown in Equation (1), the estimated distance only depends on the sound speed since light speed is several orders of magnitude higher. In order to obtain t_{arrival}, two signals with different propagation speeds are transmitted. However, several effects must be taken into account regarding timing.

- **Sequentiality**. If the signals are generated by a microcontroller or a microprocessor and some information are carried in the EM signal, then there would be a fixed delay between the emission times of both signals. Because of the deterministic nature of this situation, an easy compensation could be performed at the receiver side.
- **Channel impulse response**. In a line-of-sight situation, the direct contribution is generally dominant. Hence, the arriving signal would present a delay proportional to the distance between endpoints. However, if the situation is non–line-of-sight, the dominant contribution to the impulse response would depend on the geometry of the scenario, incurring in a distortion of the measure. Furthermore, the channel gain H(0) can highly affect the performance of the system below.
- **Noise**. The noise at the receiver might dramatically affect the system's performance, ie, the noise increases significantly the probability of a false detection of the incoming signal.

3 | SYSTEM IMPLEMENTATION

The physical implementation of the proposed system consists on building the hardware for nodes *M* and *L*, along with the development of a communication protocol and the application of a lowpass filter to mitigate the effect of ambient light noise.

3.1 | Node *M*

Figures 7 and 8 show the hardware implemented for node *M* and its schematic diagram, respectively. It consists of three main blocks, an ultrasonic transceiver, which begins the communication on the system, the optical receiver, which collects the information coming from the node *L*, and finally, the control unit that is responsible for processing the received information. The ultrasonic transmitter has an *HC-SR04* sensor, which is composed of two piezoelectric sensors: a transmitter and a receiver both in the form of a cylinder. The transmitter is responsible for emitting the ultrasonic signal and

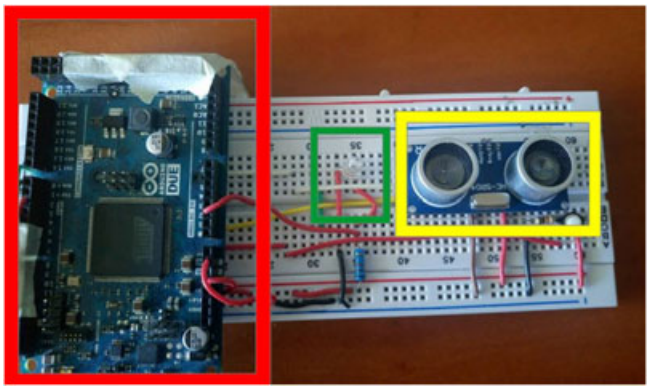

FIGURE 7 Hardware prototype for node *M*. Ultrasonic emitter (indicated by the rectangle on the right), control unit (left rectangle), and optical receiver (center rectangle)

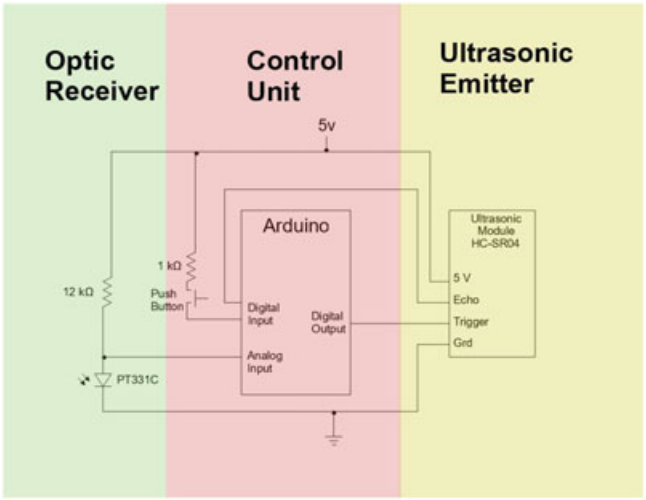

FIGURE 8 Schematic diagram for node *M*

then be bounced through an object, reaching the receiver cylinder. Assuming that the speed of sound propagation is 340 m/s, then an approximation of the distance to which an object is located can be obtained. It should be mentioned that for the node *M*, only the transmitter component of the *HC-SR04* sensor is used. On the other hand, the optical receiver is built with a *PT331C* phototransistor. This is a phototransistor with high sensibility to the infrared and visible spectrum radiation. It has a rise and fall time of 15μs, so the switching speed is sufficient for its application in the proposed system; the duration of the optical pulses is about 160 μs. The optical detection in the node *M* consists of converting the optical signal to electrical by means of the phototransistor *PT331C*, which is acquired through the ADC in the control unit. To detect the transmitted data, the ADC input signal, $V_{\text{opt}}[n]$, is compared with a predefined detection threshold $V_{\text{threshold}}$. Meanwhile, the control unit is implemented by an Arduino Due with a 32-bit ARM-cortex processor, a clock frequency of 84 MHz, and a 12-bit ADC.

3.2 | Node *L*

Node *L* comprises three main blocks as well, which are the ultrasonic receiver responsible for detecting the communication initiation with node *M*, followed by the optical transmitter used to send the reference information from node *L* to node *M*, and finally, the control unit that serves to execute the indicated actions. The hardware of the control and ultrasonic units in the node *L* are similar as those used in node *M*. In the case of the ultrasonic sensor, which is used only as a receiver component, it is necessary to physically block the transmitter sensor. This action allows the sensor to avoid the interference with itself when it is sensing the ultrasonic channel. The optical signal transmitter, $V_{tx}^{\text{opt}}(t)$, is composed of a set of five white light LEDs of 3 watts each; such transmitter has a power stage that includes a Darlington *MPSA13* transistor for each LED. The objective of this stage is to increase the current in the LED and consequently the luminosity

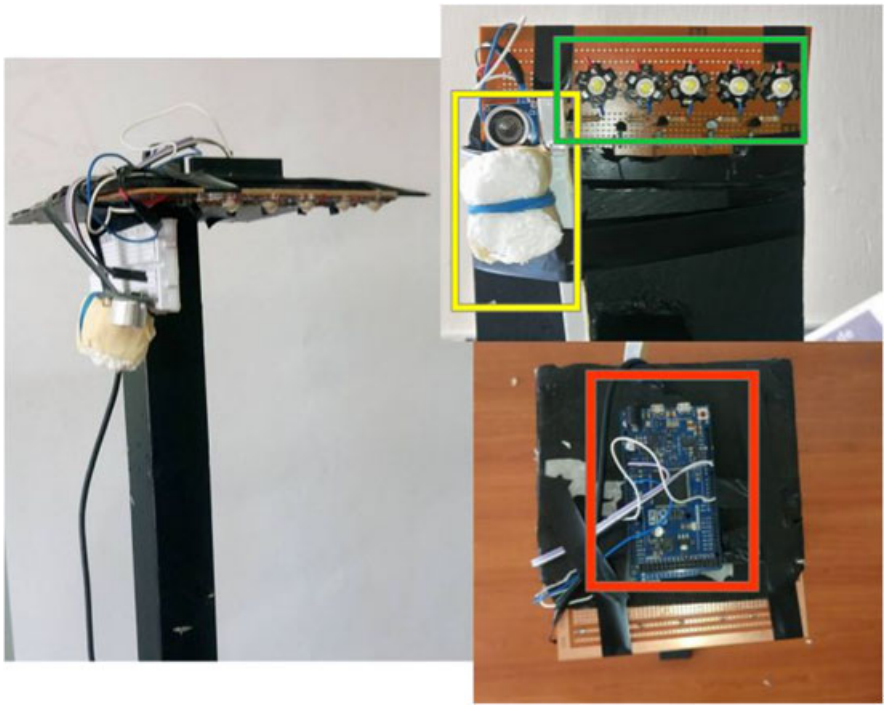

FIGURE 9 Hardware prototype for node *L*. Ultrasonic receiver (indicated by the upper left rectangle), control unit (bottom rectangle), and optical transmitter (upper right rectangle)

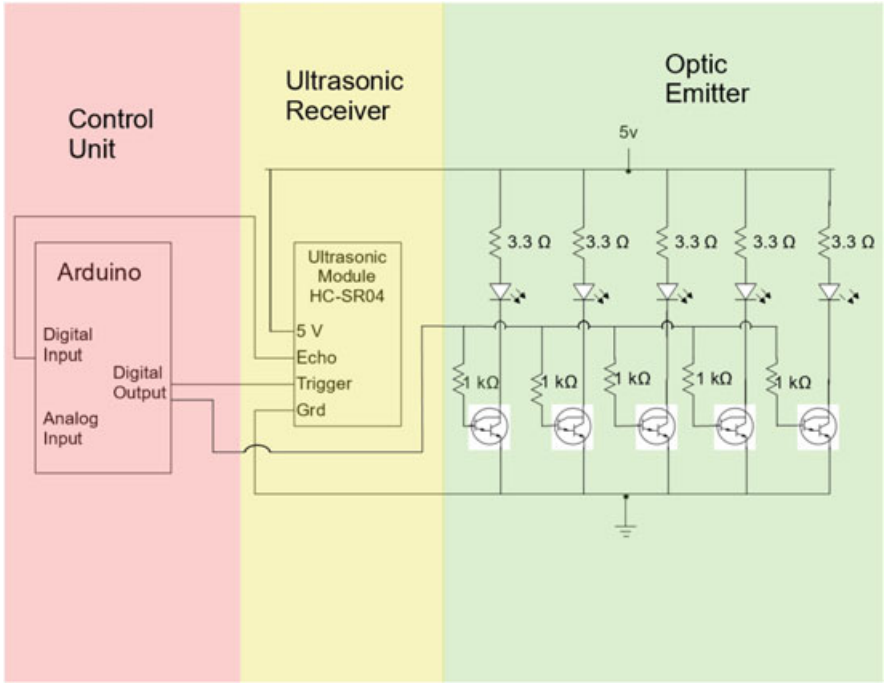

FIGURE 10 Schematic diagram for node *L*

level of the source and, with it, the coverage of the system. Figure 9 shows the hardware implemented for node *L*, and Figure 10 shows the corresponding schematic diagram.

3.3 | Communication protocol

Once the node *L* detects the ultrasonic signal coming from node *M*, it proceeds to initiate the optical communication process. In order to carry out this process, it is necessary to implement a specific connection protocol. In this case, our

SYN (8 bits)								ACT (4 bits)				ID (12 bits)												SLOT (6 bits)						SCS (1bit)	FCS (1bit)
1	0	1	0	1	0	1	0	1	1	1	1	0	0	0	0	1	0	1	1	0	0	0	1	0	0	1	1	1	1	0	0

FIGURE 11 Frame format for the proposed communication protocol

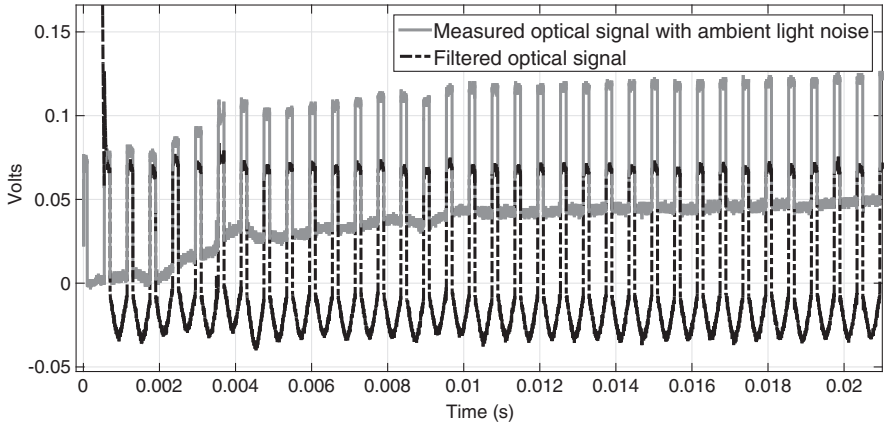

FIGURE 12 Illustration of the ambient light noise reduction filter applied to the optical received signal at node *M*

protocol has a frame with fixed length of 32 bits; this format has been adapted from the IEEE 802.15.7 standard. The frame size is selected with the purpose of avoiding long periods of time during the transmission since node *M* has a limited speed to process the information. In addition, the larger the value of t_{frame}, the greater must be $t_{r,L}$ to prevent the probability of collision on the optical channel. On the proposed system is necessary to take on consideration the t_{frame} because if t_{frame} increases, $t_{r,L}$ will be increased too. The period $t_{r,L}$ is the time necessary on the node L transmission for multiple access scheme to avoid collisions. The proposed frame format can be seen in the Figure 11.

The system uses a type of time division multiple access system to avoid collisions; each node L has a specific delay in the optical communication channel denoted by $t_{r,L}$. Each node L has a specific transmission delay after receiving the ultrasonic signal; the delay could have a fixed value between 5 to 50 milliseconds in multiples of 5 milliseconds. This time information is allocated on the *SLOT* space of the frame format. Other important field in the frame is the *ID* space which serves for node *M* to identify the node *L* that is sending the frame. Finally, when the optical communication process is completed, the time is stored and subtracted from the processing time, t_{rx}^{p}, and from the access time to the medium, $t_{r,L}$, to calculate the node distance. When node *M* has three estimated distances from different nodes and the communication time limit t_4 has finished, we proceed to perform the trilateration method to determine the location of node *M*.

3.4 | Ambient light noise reduction

Because of the changes of the surrounding light intensity in a typical room, we first require to reduce the distortion of the ambient light noise in the optical link before evaluated the positioning system. Figure 12 shows the effect of ambient light at the receiver of Node *M* using an *OOK* modulated optical signal (solid line) in a typical environment of an office room. The ambient light contribution behaves like an offset signal that changes gradually over time. It can be seen that the light noise component has a low frequency contribution; therefore, it can be removed by a digital lowpass filter. To overcome this distortion, we applied a lowpass filter with a cutoff frequency of 100 MHz. The filter order and cutoff frequency were setup using a trial and error approach. Figure 12 presents the results after filtering the measured optical signal (dash line).

4 | EXPERIMENTAL RESULTS

The experimental validation of the proposed VLC-based localization system was carried out during a typical day in an office room with several windows. Figure 13 shows the scenario under consideration. It includes a 100 (cm) ×100 (cm) ×100 (cm) space with 4 nodes L with positions in $N_{L1} = (0, 0, 90)$, $N_{L2} = (0, 100, 90)$, $N_{L3} = (100, 0, 90)$, and $N_{L4} = (100, 100, 90)$. Node *M* can be placed at any point within the square surface marked on the table in Figure 13, that is, $N_M = (X, Y, 0)$, where $0 \leq X, Y \leq 100$ cm. As a reference, it can be seen that the lower left corner of the marked

FIGURE 13 Scenario under consideration for the experimental validation of the proposed visible light communication–based indoor localization system

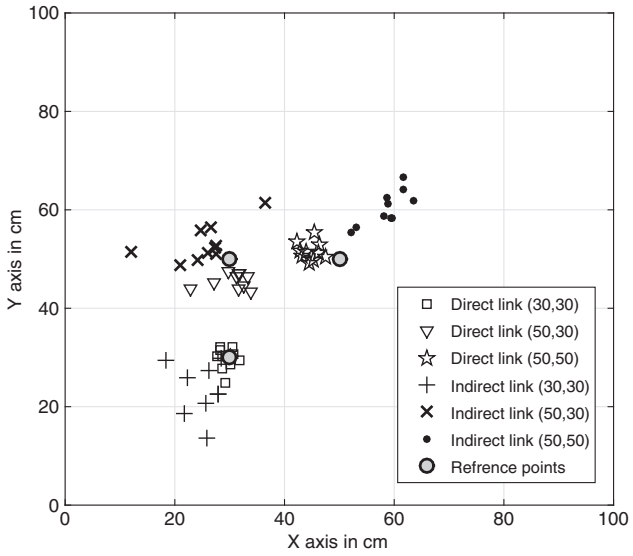

FIGURE 14 Measurement results for the proposed localization system

area represents the origin, $O = (0, 0, 0)$, of the coordinate system. The mitigation of ambient light noise is performed by applying a lowpass filter of order 200 with a cutoff frequency of 100 MHz. The system transmission rate was set to 6.25 kbps.

The system is evaluated for 3 different locations of node M using the scaled scenario presented in Figure 13. These positions are (30,50,0), (50,50,0), and (30,30,0), which are marked on the scenario. The nodes L are assumed to be placed on a pedestal at a height of 90 cm. Without loss of generality, a sequential measurement method is performed to allow the transmissions at least of three nodes L with the same physical device but at different instants of time. As a first step, we carry out the communication process between node M and node L_1; next, we proceed by moving the pedestal to the location of node L_2, where the same process is performed again. Finally, this same procedure is performed with the node at location L_3. When obtaining the information of three nodes L, we estimate the location of the node M through the trilateration method.

Figure 14 presents the measurements results for the three locations of node M. Two different measurements are taken for each of the locations. In the first case, the ultrasonic sensors at node M and node L are aligned (direct link), whereas in the second case, they are misaligned (indirect link), for the latter, the direction of the ultrasonic sensor at node M is pointed to the roof forming a 90 ° angle with the floor. In both cases, the ultrasonic sensor from node L has a direction to the floor. As expected, the results show a greater error margin when the ultrasonic sensor was not aligned; however, even on these cases, the error on localization estimation are on a satisfactory range, within a radio of 10 cm for the direct link cases and 20 cm for the indirect links. It was observed that the main factor affecting the localization estimates was the propagation attenuation and the angle of reception for the ultrasonic signal.

Further results are presented in Table 1. We perform another 10 independent measurements per each location and calculate again the distance error between the estimated and real positions, with both direct and indirect links. According

TABLE 1 Distance errors obtained in the experimental results of the proposed visible light communication–based indoor localization system

Direct Link Localization Errors			
Position	**Average**	**Minimum**	**Maximum**
(30,30,0)	2.2888	0.8965	5.1515
(30,50,0)	5.1266	2.4542	9.3595
(50,50,0)	5.7634	2.4725	8.5341
Indirect Link Localization Errors			
Position	**Average**	**Minimum**	**Maximum**
(30,30,0)	8.2665	0.2554	16.8628
(30,50,0)	8.1757	2.6780	20.0481
(50,50,0)	12.5809	5.8701	20.3940

TABLE 2 Comparative summary of indoor positioning systems methods

Ref.	Type of Results	Method	Measurement Quantity	Signal Processing	Average Error
13	Simulated	Triangulation	Pixels Distance	High	20 cm with image 2000 x 1500 px
6	Simulated	Triangulation & Trilateration	RSSI & Angle Diversity	Low	11 cm
9	Simulated	Trilateration	RSSI	Medium	16 cm
8	Experimental	Trilateration	RSSI	High	Less 5 cm
10	Experimental	Trilateration	RSSI	High	4 cm
11 and 12	Experimental		RSSI	High	56 cm
7	Experimental	Trilateration	RSSI	Low	
Proposed	Experimental	Trilateration	RTOF	Low	6 cm

Abbreviations: RSSI, received signal strength intensity; RTOF, round-trip time of flight.

to these results, the differences between direct and indirect links results are meaningful. It was observed that the main factor affecting the localization estimates was the propagation attenuation and angle of reception for the ultrasonic signal. The average error on direct link were less than 6 cm, but on indirect link, it increased up to 20 cm. Notice that position (50, 50, 0) yields the highest error; this is because the distance between the two ultrasonic sensors are the largest, and the directivity between the ultrasonic emitter and receiver is lower.

Finally, Table 2 provides a comparative summary of the most relevant VLC-based indoor positioning systems in the literature with the proposed system. In particular, we observe that the proposed system can be as accurate as other experimental methods but with the advantage of demanding low signal processing blocks. Moreover, it requires an easy setup process to perform localization; basically, it needs the information of the space positions of the nodes *L*. On the other hand, the most complex task is carried out by node *M* during the detection process of the data frame sent by the nodes *L*.

5 | CONCLUSIONS

The experimental implementation of a VLC-based indoor localization system was presented in this paper. The system was built using a hybrid communication system where a VLC connection was performed in the downlink and an ultrasonic connection in the uplink. The experimental results show that the proposed system achieves a good tradeoff between precision and implementation complexity yielding low error estimates. However, it is found that the system is sensitive to the ambient light noise and the alignment of the ultrasonic sensors (transmitter and receiver). While the proposed VLC-based localization system benefits from a simple structure (with low-cost commercial components) whose results are appealing, future work includes the use of more advanced signal processing methods to improve the robustness and coverage of the system to ambient light but at the expense of adding more hardware capacity. In addition, a scheme for medium sharing have to be issued to assure that the nodes ultrasound emissions are not overlapped for multiple nodes localization.

ACKNOWLEDGMENTS

This work was supported in part by CONACYT, Mexico under grant 236188 and by the Spanish Government (Economy, Industry and Competitiveness Ministry) as a part of the Spanish National Research Plan (ARIES Project Ref. TEC2013-47682-C2-1).

CONFLICT OF INTEREST

The authors declare no potential conflict of interests.

ORCID

E. Torres-Zapata http://orcid.org/0000-0002-6572-3889
J. M. Luna-Rivera http://orcid.org/0000-0002-2694-0012

REFERENCES

1. Pathak PH, Feng X, Hu P, Mohapatra P. Visible light communication, networking, and sensing: a survey, potential and challenges. *IEEE Commun Surv Tutor*. 2015;17(4):2047-2077.
2. Liu H, Darabi H, Banerjee P, Liu J. Survey of wireless indoor positioning techniques and systems. *IEEE Trans Syst Man Cybern Part C*. 2007;37:1067-1080.
3. Song J, Ding W, Yang F, et al. Indoor hospital communication systems: an integrated solution based on power line and visible light communication. Paper presented at: 2014 IEEE Faible Tension Faible Consommation; 2014; Monaco, Monaco.
4. Hamza AS. Optical wireless communications airport surface operations: opportunities and challenges. Paper presented at: 2016 Integrated Communications Navigation and Surveillance; 2016; Herndon, VA.
5. Iturralde D, Seguel F, Soto I, Azurdia C, Khan S. A new VLC system for localization in underground mining tunnels. *IEEE Lat Am Trans*. 2017;15(4):581-587.
6. Yin L, Wu X, Haas H. Indoor visible light positioning with angle diversity transmitter. Paper presented at: 2015 IEEE 82nd Vehicular Technology Conference; 2015; Boston, MA.
7. Sharifi H, Kumar A, Alam F, Arif KM. Indoor localization of mobile robot with visible light communication. Paper presented at: 2016 12th IEEE/ASME International Conference on Mechatronic and Embedded Systems and Applications (MESA); 2016; Auckland, New Zealand.
8. Guo X, Shao S, Ansari N, Khreishah A. Indoor localization using visible light via fusion of multiple classifiers. *IEEE Photonics J*. 2017;9(6):1-16.
9. Wang L, Guo C, Luo P, Li Q. Indoor visible light localization algorithm based on received signal strength ratio with multi-directional LED array. Paper presented at: 2017 IEEE International Conference on Communications Workshop; 2017; Paris, France.
10. Cai Y, Guan W, Wu Y, Xie C, Chen Y, Fang L. Indoor high precision three-dimensional positioning system based on visible light communication using particle swarm optimization. *IEEE Photonics J*. 2017;9:1-20.
11. Qiu K, Zhang F, Liu M. Visible light communication-based indoor localization using Gaussian process. Paper presented at: 2015 IEEE/RSJ International Conference on Intelligent Robots and Systems; 2015; Hamburg, Germany.
12. Qiu K, Liu M. Visible light communication-based indoor environment modeling and metric-free path planning. Paper presented at: 2015 IEEE International Conference on Automation Science and Engineering; 2015; Gothenburg, Sweden.
13. Huynh P, Lee J, Yoo M. An indoor environment VLC-based localization algorithm for handset devices. Paper presented at: 2015 Seventh International Conference on Ubiquitous and Future Networks; 2015; Sapporo, Japan.
14. Marin-Garcia I, Chavez-Burbano P, Muñoz-Arcentles A, Calero-Bravo P, Perez-Jiménez R. Indoor location technique based on visible light communications and ultrasound emitters. Paper presented at: 2015 IEEE International Conference on Consumer Electronics (ICCE); 2015; Las Vegas, NV.

How to cite this article: Torres-Zapata E, Luna-Rivera JM, Perez-Jimenez R, et al. Implementation of a VLC-based indoor localization system. *Trans Emerging Tel Tech*. 2019;30:e3498. https://doi.org/10.1002/ett.3498